ESRF	**Experiment title:** **"Dependence of the magnetic anisotropy in low-dimensional Fe structures on Fe-Pt coordination"**	**Experiment number**: HE-1965
Beamline: ID 08	**Date of experiment**: from:　14/09/2005 at 16:00　　to:　20/09/2005 at 8:00	**Date of report**: 18.1.2006
Shifts:	**Local contact(s)**: Dr. Peter Bencok	*Received at ESRF:*

Names and affiliations of applicants (* indicates experimentalists):

J. Honolka[¶,*], A. Enders[¶,*], K. Kuhnke[¶,*], D. Repetto[¶,*], V. Sessi[¶,*], K. Kern[¶]

[¶] *Max-Planck-Institut für Festkörperforschung, 70569-Stuttgart, Germany.*

Report:

The aim of this project was to study the dependence of the magnetism of low-dimensional Fe structures on the interaction with Pt on the atomic scale. For this purpose we prepared several Fe structures where the number of nearest Pt neighbors per Fe atom, NN_{Pt}, was systematically increased from $NN_{Pt} = 3$ to $NN_{Pt} = 12$. Such experiments directly adress the origin of large magnetic anisotropy in FePt alloys and may thus be useful for the development of nanostructures with extreme magnetic properties. We found out within the project HE-1965 that indeed the Fe-Pt coordination drives the magneto-crystalline anisotropy energy (MAE) via hybridization effects. Most unexpectedly though we could also find evidence for a non-collinear spin alignment of neighbouring Fe atoms with increasing Fe-Fe coordination. MAE and magnetic moment per atom are thus determined by the balance of the Fe-Fe and Fe-Pt coordination effects, as will be shown in this report.
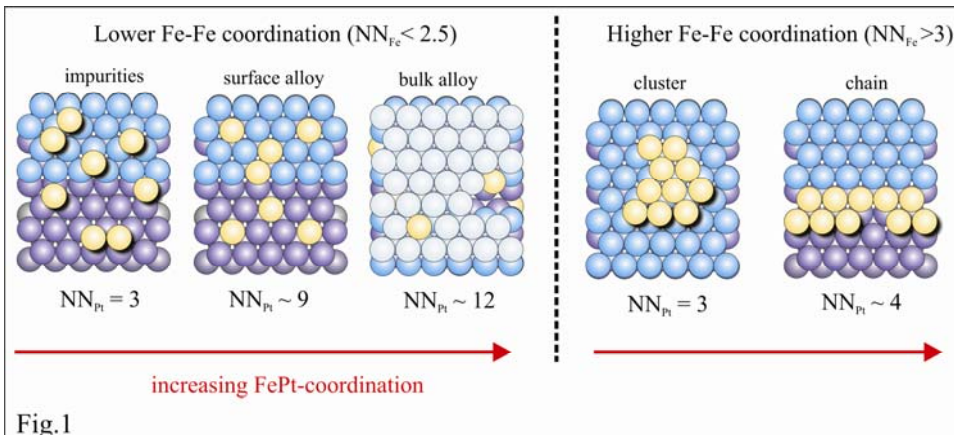

Fig.1

Five different samples sketched in the Fig.1 were prepared *in situ* under UHV conditions using our experience in the growth of low-dimensional Fe structures on vicinal Pt(997) surfaces [1]. The growth conditions and nominal Fe coverages are listed in Table 1. Impurities on the surface were prepared by deposition of Fe atoms onto a cold substrate with T ~ 10K to prevent coalescence.

Upon raising the substrate temperature the Fe atoms are able to diffuse to the steps and form chains. With further increase of the temperature during growth the Fe atoms will first diffuse into the topmost monolayer of Pt and above 600K into the bulk. The cluster sample was grown on Pt(111) at room temperature where Fe atoms coalesce to form larger 2D islands. In Fig.1 the samples are divided into two groups with low and high average Fe-Fe coordination, NN_{Fe}. Within the two groups the average number of next neighbor Pt atoms per Fe atom, NN_{Pt}, increases from left to right as indicated by the red arrow.

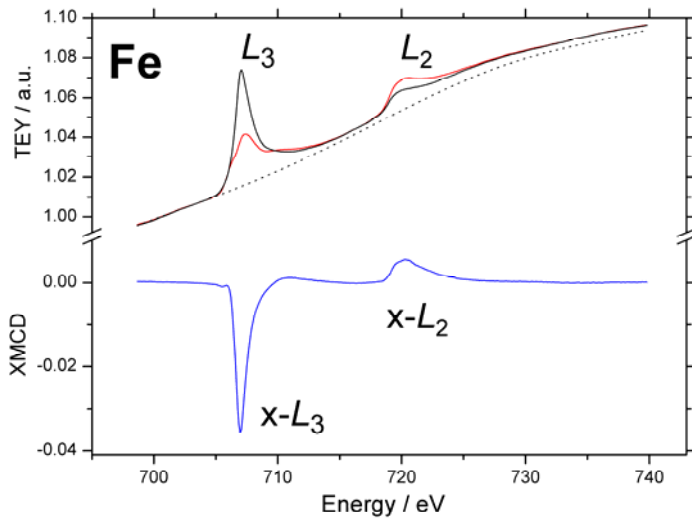| **Table 1**	growth temperature	coverage	substrate
impurities	10 K	0.31 ML	Pt(997)
surface alloy	600 K	0.29 ML	Pt(997)
bulk alloy	550 K	0.28 ML	Pt(997)
cluster	300 K	0.26 ML	Pt(111)
chain	300 K	0.28 ML	Pt(997)

Fig. 2

X-ray absorption spectra (XAS) at the Fe $L_{3/2}$ edge (between 690eV and 740eV) were recorded as a function of angle θ with the surface normal. Typical XAS spectra for positive and negative circular polarization are shown in Fig.2 together with the Pt background derived from a measurement on a pure Pt substrate (black dotted line). The spectra are taken in a maximum field of 5.5 Tesla which leads to the X-ray magnetic circular dichroism (XMCD) signal shown in the lower panel.

Along selected orientations magnetic hysteresis curves were measured by ramping the magnetic field and normalizing the L_3 peak intensity to the intensity at energies just below the onset of the L_3 edge. The plots are shown in Fig.3 for $\theta = 0°$ (red)
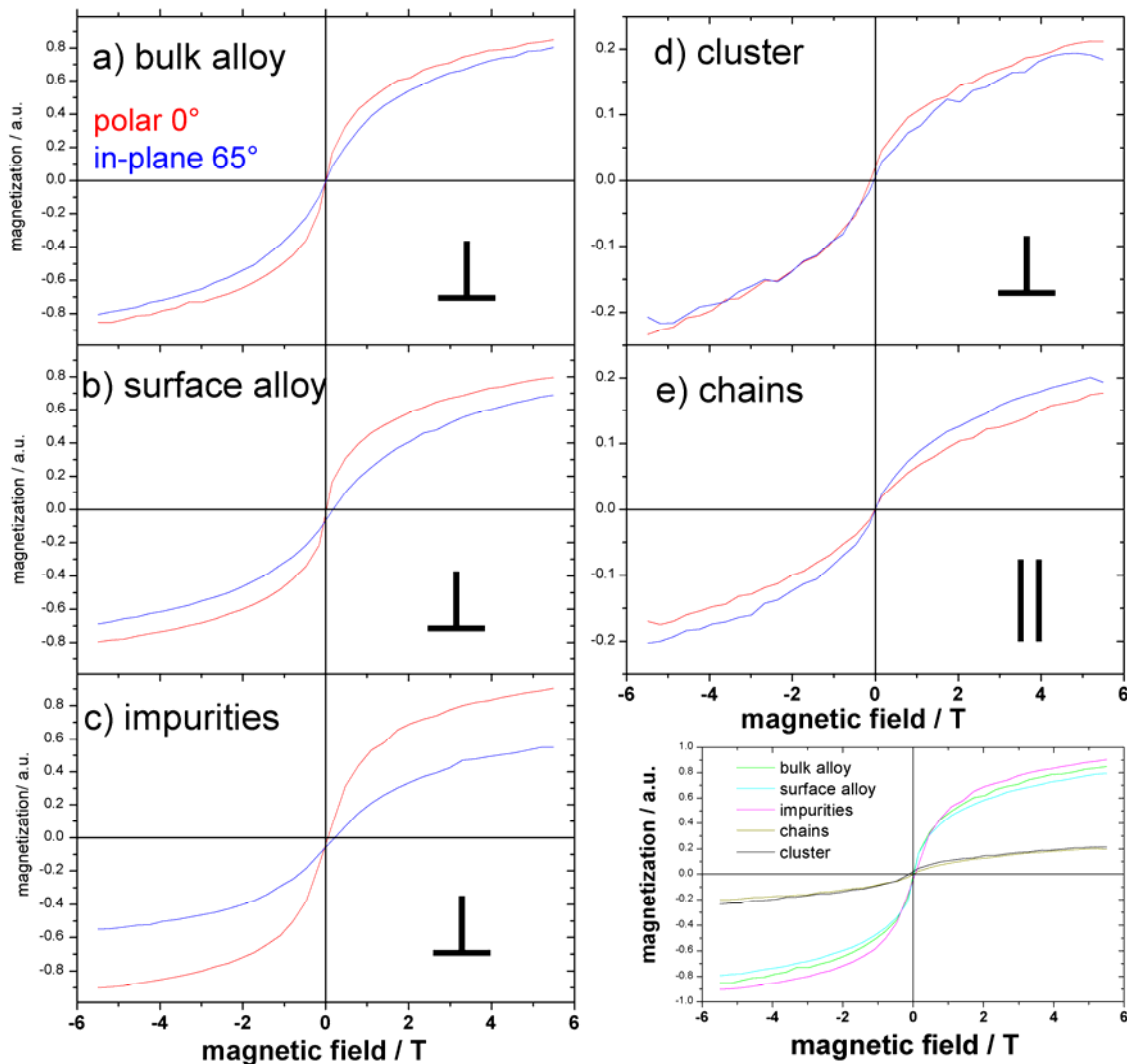

Fig.3

and $\theta = 65°$ (blue) both directions being perpendicular to the substrate step direction [$\bar{1}10$]. All samples show an out-of plane magnetization easy axis except of the chains which preferentially align in-plane. Fig.3 gives an overview over the directional dependence of the hysteresis loops of all samples. The left block, Fig. 3(a), 3(b) and 3(c), shows the samples with low NN_{Fe} coordination. A clear decrease of the magnetic anisotropy is seen when NN_{Pt} increases. For the high Fe-Fe coordination samples, Fig. 3(d) and 3(e), the anisotropy is generally low and vanishes nearly completely for the cluster sample. In the lower right plot the loops of all samples along their easy axis direction are shown for comparison. A striking collaps of the magnetization by about a factor 4 is observed when going from low to high Fe-Fe coordination samples. Oxidation effects were excluded by monitoring the O-K absorption lines of each sample before and after the

measurements. From the Fe $L_{3/2}$ spectra taken in a field of $H = 5.5T$ the effective spin and orbital moments per hole, $(m_S + m_T) / n_h$ and m_L / n_h were deduced using the sum rules[2]. The measured Pt-background (dotted line in Fig. 2) and a step-like $2p$-$4s$ contribution was substracted to derive the integral of the non-dichroic XAS. In Fig. 4 the spin and orbital moments are plotted versus t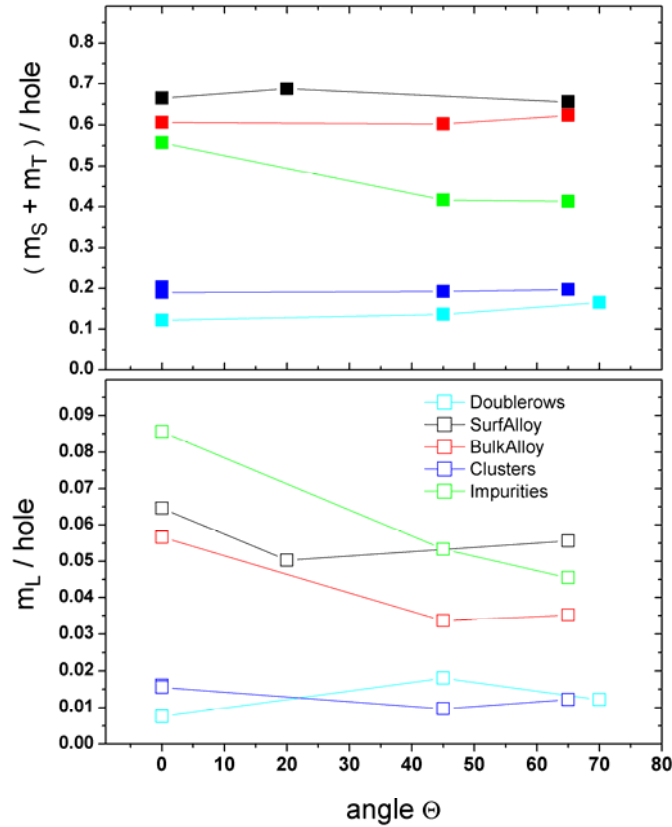he angle of incidence θ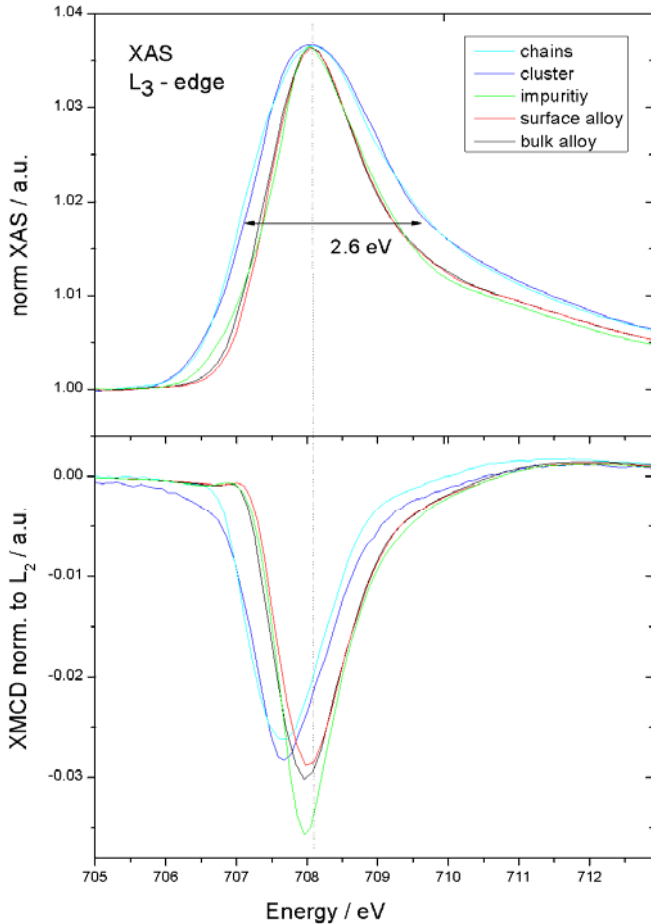. At $\theta = 0°$, $(m_S + m_T) / n_h$ of the high-spin samples correspond to spin moments per Fe-atom between 1.8 and $2.2\mu_B$ assuming $n_h = 3.3$. For the impurity sample the spin moment drops towards the hard magnetic axis (higher angles θ) due to incomplete saturation. This is not the case for all other samples where the magnetic anisotropy is considerably smaller. The spin moments per Fe atom for clusters and chains along their easy magnetic axis are considerably smaller (0.65 and $0.54\mu_B$ per Fe atom, respectively). Interestingly, this spin-transition goes along with changes in the shape of the XAS and XMCD signals as shown in Fig. 5, where the L_3-absorption edges of all samples are shown in detail. For a better comparison the XAS curves of all samples have been normalized to their L_3 maximum value. For the XAS absorption lines of the low-spin samples a FWHM of 2.6eV is found, which is about 40% broadened compared to the ones with a high spin. For comparison: A 4ML Fe-film grown on Pt(111) has an even larger FWHM of 3.1eV. Also the magnetic XMCD signals normalized to their L_2 peaks in the lower panel clearly indicate changes in the electronic states of the Fe atoms: The XMCD peak has shifted to lower energies for the high Fe-Fe coordination samples. We thus interpret the broadening in the XAS signal as a consequence of increased Fe-Fe coordination. While NN_{Fe} has a large influence on the electronic structure, NN_{Pt} seems to leave it more or less unaffected. This is most obvious when comparing the bulk alloy with the impurities sample where in the ideal case NN_{Pt} is 12 and 3, respectively.

Like the spin-moments also the orbital moments of clusters and chains are reduced compared to the high spin samples along the easy axis direction. The reduction is of the same order as found for the spin moments. Nevertheless, m_L clearly exhibits changes with the angle θ. The orbital moment of the impurity sample decreases with increasing direction away from the easy axis (Incomplete saturation can only in part account for this effect as can be seen in the angular dependence of the spin-moments). This could be interpreted using P. Bruno's approximation $\Delta E_{MAE} \propto -\Delta m_L$ [3], where ΔE_{MAE} is the magneto-crystalline anisotropy. However, for the other high-spin samples m_L shows a weak non-monotonous behavior despite the fact that they clearly exhibit only one single magnetic easy axis at $\theta = 0°$ in the range of $\theta = [-65°, 65°]$. It thus seems that Bruno's Ansatz does not strictly hold for these systems. For a better understanding this result needs to be compared with

Fig. 4

Fig.5

theoretical calculations. It is however known that in FePt alloys the hybridization of Fe-3d and Pt-5d states are of great importance for the magnetic anisotropy. According to the latest calculations in these systems the magnetic anisotropy is caused by the strong spin-orbit coupling constant of the Pt which pertubates the Fe-states due to hybridization. This mechanism is distinctively different from Bruno's model, which is based on the spin-orbit coupling of the Fe only. The fact that the cluster sample shows a vanishing MAE although from a viewpoint of symmetry it should behave similar to the surface alloy sample supports the importance of NN_{Pt}.

For an understanding of the occurance of the low-spin phase in cluster and chain samples one needs theoretical modeling of small clusters of Fe on Pt substrates. The effect can be either due to a reduction of the spin moment for every Fe atom ("true" low-spin phase) or due to uncompensated antiferromagnetism. We want to stress the fact that the cluster and chain samples do not show a decreased branching ratio $L_3/(L_3 + L_2)$ compared to the other samples. According to theory [4] the reduction of the spin polarization caused by hybridization and crystal field effects is associated with a decrease of the branching ratio. We therefore tend to believe that the observed low spin moments are either due to an antiferromagnetic coupling between Fe atoms or partial canting of Fe moments.

The stability of m_L with increasing NN_{Pt} is noteworthy: Even for the bulk alloy sample the highly coordinated Fe carries an orbital moment of about $0.19\mu_B$. For comparison orbital moments of $0.07\mu_B$ are obtained in bulk bcc-Fe. It has been shown recently that 3d metal orbital moments may survive in bulk Au hosts, which has similar lattice paramters as Pt[5]. The unquenching of the orbital moments is reported to depend on a delicate balance of hybridization effects between the local 3d metal with the host and the filling of the 3d states of the 3d metal. However, the fact that Pt has a much larger DOS at the Fermi level compared to Au should alter the quenching mechanism. Comparing the orbit-spin magnetic moment ratio found for Fe in a Au host [5] (0.034) with the one of our bulk alloy sample (0.094) it seems that in our case the quenching mechanism is even weaker. We want to stress at this point that due to the statistical diffusion of Fe atoms into the bulk during the preparation of the bulk alloy sample there will be a small fraction of less coordinated Fe atoms in the topmost Pt layer with $NN_{Pt} = 9$ which contribute to the magnetic properties.

[1] T.Y.Lee et al. (2004) submitted.
[2] B. T. Thole et al. Phys. Rev. Lett. **68**, 1943 (1992), P. Carra et al. Phys. Rev. Lett. **70**, 694 (1993).
[3] P. Bruno, Phys. Rev. B **39**, 865 (1989)
[4] B. T. Thole, G. van der Laan, Phys. Rev. B **38**, 3158 (1988),
[5] W.D. Brewer et al. Phys. Rev. Lett. **93**, 77205 (2004).